Eur. Phys. J. B **53**, 99–108 (2006)
DOI: 10.1140/epjb/e2006-00351-2

THE EUROPEAN PHYSICAL JOURNAL B

Finite size effects on the optical transitions in quantum rings under a magnetic field

T.V. Bandos[a], A. Cantarero, and A. García-Cristóbal

Material Science Institute, Universitat de València, PO Box 22085, 46071 Valencia, Spain

Received 23 May 2006 / Received in final form 29 July 2006
Published online 22 September 2006 – © EDP Sciences, Società Italiana di Fisica, Springer-Verlag 2006

Abstract. We present a theoretical study of the energy spectrum of single electron and hole states in quantum dots of annular geometry under a high magnetic field along the ring axis in the frame of uncorrelated electron-hole theory. We predict the periodic disappearance of the optical emission of the electron-hole pair as the magnetic field increases, as a consequence of the finite height of the barriers. The model has been applied to semiconductor rings of various internal and external radii, giving as limiting cases the disk and antidot.

PACS. 73.21.La Quantum dots – 71.35.Ji Excitons in magnetic fields; magnetoexcitons – 73.23.Ra Persistent currents – 78.67.Hc Quantum dots

1 Introduction

The Aharonov-Bohm (A-B) oscillations [1] in mesoscopic metallic and semiconductor rings have attracted much interest and have been studied both experimentally [2–4] and theoretically [5–10]. The A-B quantum interference effect in such systems arises from the phase shift accumulated by the wave function of a charged particle moving in a ring pierced by an external magnetic field.

Recently, magneto-transport experiments have been complemented by the detection of the A-B signature through optical properties of mesoscopic rings [11,12]. Since it has become possible to manufacture self-assembled semiconductor quantum dots with ring shape there have been considerable efforts to develop spectroscopic tools capable to detect the energy spectrum in a magnetic field because of their high optical quality [13]. Ring-like properties of few electrons in self-assembled quantum dots under a magnetic field have been studied by far-infrared spectroscopy [14].

The main physics of the A-B optical oscillations for magneto-exciton was predicted in quantum rings (QRs) [9,15]. The elementary neutral excitation, the so-called *neutral* exciton, is a bound state of a hole in a filled valence band and an electron in an otherwise empty conduction band of the host semiconductor. The A-B effect in a semiconductor quantum ring for charged particle has recently been studied in optical experiments [11], while for neutral exciton it has not been observed yet in type-I QRs.

Govorov et al. [16–18] have considered the possibility to detect optically an A-B signature for a polarized electron-hole (e–h) pair in a quantum ring of finite width. An essential feature of their study is the radial polarization, incorporated by the modeling of the neutral exciton with and without Coulomb interaction in the QR as two concentric parabolic rings for the electron and hole. In both limiting cases of strong and weak interaction, the radial polarization allows for the optical manifestation of the topological A-B effect for neutral exciton in a finite width ring, in contrast with the exponentially small amplitude of the A-B oscillations of the ground state energies in "zero" width quantum rings [9,10,19,20]. Recently, the A-B effect was studied for spinless interacting hole and electron within the frame of attractive Hubbard model on the discrete lattice of the few rings in vacuum [21]. One can state that this paper, like [9,10,19,20], takes into account e–h Coulomb interaction, but by modeling it by the exactly soluble Hubbard Hamiltonian (e.g. in [10] the delta-function potential is used instead). The conclusions in [21] include that the A-B effect is suppressed when the QR circumference becomes large, whereas it is due to the large width in accordance to [20]. It was also noted in [21] that the phenomenon in the two-dimensional (2D) model is analogous to one in the one-dimensional (1D) system. This is the place to notice that both A-B and Aharonov-Casher [22] effects in the N-fermion Hubbard model with attraction at the 1D ring lattice under a radial electric field have been studied in [23] (see also [24]). The enhancement of A-B effect due to external electric field in the 2D ring was studied in [25].

The interplay between the excitonic radial polarization and Coulomb interaction was analyzed in [26,27],

[a] e-mail: Tatyana.Bandos@uv.es

assuming that the hole and electron are restricted to 1D concentric rings. Here we consider non-interacting electron and hole both in the 2D ring immersed in a matrix of host semiconductor. Such a simple model allows us to study tunneling effect through finite height potential (instead of infinite potential as, e.g. in [19]). The height of the hard wall potential influences the angular momentum transitions [28] which are one of the subjects of our main interest. It has been proposed that type-II quantum dots, where one charged particle is located inside the quantum disk, whereas the other one is localized outside, enables to reveal A-B oscillations with increasing magnetic field [15,28]. According to this prediction, the optical A-B effect has only recently been observed for polarized e–h pairs in type-II self-assembled quantum dots [12]. In such a type-II quantum disk, but with finite thickness, where a single particle can be found above or below the disk, the angular momentum transitions in a perpendicular magnetic field were studied in [29]. In order to explain why the A-B photoluminescence (PL) of neutral exciton has not yet been detected in type-I semiconductor quantum rings [30], the model [16] needs further refinement. We consider a two-dimensional quantum ring that has a different finite depth potential well of the same width for the electron and hole without making an assumption about the electron-hole spatial separation (polarization). Our interest in the finite size effects has been motivated by the prospect that the optical and electronic properties of self-assembled structures can be designed (by reduction of potential depth and variation of geometry parameters) to allow for the optical observation of the A-B quantum interference at low temperatures.

It is shown from the energy spectrum of an e–h pair in a finite width quantum ring that the photoluminescence emission exhibits a periodic disappearance with the magnetic field. We discuss the undetectability of the A-B oscillations for neutral exciton as due to the very small magnetic field intervals where the PL signal is absent. In our study, we consider strain free QRs. Such objects, namely unstrained GaAs quantum dots, were recently fabricated by novel self-assembly technique [31,32]. The intervals in magnetic field, for which the photoluminescence is suppressed, are calculated here numerically, and some related expressions have been derived semiclasically. We do not consider Coulomb interaction between electron and hole in a finite width QRs. In the literature the periodic disappearance of the optical signal from QRs has been mainly studied in the extreme limits of weak and strong electron-hole correlation [16–18,21,26,27,33]. As it was shown in [26], the A-B effect remains only in the case of weak interaction and radial polarization, though this is still under discussion [27]. The periodic change of the ground state angular momentum in magnetic field is more pronounced in the case of interaction screening and if the electron is assumed to be closer to the center of the QR [26]. Our two-dimensional model do not need in such assumption and also allows to take into account the penetration of magnetic field into the material of ring, which is common for all experiments. In the present work we model the quantum ring by an annulus with zero thickness along the growth direction; this in-plane confinement is a rather characteristic feature for the semiconductor rings produced by modern technology.

The paper is organized as follows. In Section 1, we present the basic equations and the general procedure to obtain the energy spectrum of a charged particle in a QR under a magnetic field. In Section 2, we calculate numerically the eigenenergies and wavefunctions by solving the secular equation, estimate the e–h pair overlap integral by employing the single-particle wave functions and represent our results in form of phase diagrams of angular momentum transitions for rings of various widths. In Section 3 we discuss semi-classically the tunneling through finite height hard walls of QRs. In Section 4, we present our conclusions. Appendix A contains QR finite width corrections to the Landau energy at high magnetic fields.

2 Theoretical model

We consider an electron (or hole) in a QR with a magnetic field B applied normally to the plane of the ring. We assume the motion to be strongly limited along the z direction and, therefore, only consider the two-dimensional in-plane motion. Moreover, the Coulomb interaction between the electron and hole is ignored in a first approximation. The problem is thus reduced to one for two independent particles, electron and hole, with opposite charge and different effective masses, confined by barriers of different height. Then the boundary problem for the e–h pair in a magnetic field becomes exactly solvable. Spin coupling effects are also neglected.

The in-plane motion of a charged particle in a quantum ring under a perpendicular magnetic field is limited by the boundary conditions imposed by the nanostructure, whereas the magnetic field introduces a structure independent quantization. Although the parabolic-like confinement potential is one of the most commonly used approximation for some QRs [4,8,34] (in particular, because it allows the Fock-Darwin solution for energy eigenvalues in an explicit form [35]), a realistic potential acting on the carriers might differ significantly. The parabolic confining potential model has been used to study the magnetic-field-induced suppression of the photoluminescence [16]. We assume here that a finite hard wall potential limits the motion of the electron and hole in the same radial range, but with different barrier heights, and show that it causes the radial polarization of the e–h pair. Another peculiarity of our approach is the existence of unbound states: the finite size potential of the QR in our approximation allows to take them into consideration as well, in contrast to the parabolic and infinite hard wall models.

Within the above model, due to the axial symmetry, the Hamiltonian of a charged particle is invariant under spatial rotation about the z axis that passes through the center of the QR. Therefore, it follows the conservation of the projection of the angular momentum on the z axis, l_z,

$$\begin{vmatrix} M(\nu_{ex},b;r_1^2/2) & U(\nu,b;r_1^2/2) & M(\nu,b;r_1^2/2) & 0 \\ M'(\nu_{ex},b;r_1^2/2) & U'(\nu,b;r_1^2/2) & M'(\nu,b;r_1^2/2) & 0 \\ 0 & U(\nu,b;r_2^2/2) & M(\nu,b;r_2^2/2) & U(\nu_{ex},b;r_2^2/2) \\ 0 & U'(\nu,b;r_2^2/2) & M'(\nu,b;r_2^2/2) & U'(\nu_{ex},b;r_2^2/2) \end{vmatrix} = 0. \quad (5)$$

for both electron and hole, and the wave function can be generally factorized as

$$\Psi(\rho,\varphi) = \frac{e^{il\varphi}}{\sqrt{2\pi}} R(\rho), \quad (1)$$

where $l = 0, \pm 1, \pm 2 \ldots$ is the quantum number determining the angular momentum $l_z = l\hbar$.

The radial function $R(\rho)$ obey the Schrödinger-like equation:

$$\left[-\frac{\hbar^2}{2m}\frac{1}{\rho}\frac{\partial}{\partial\rho}\left(\frac{1}{\rho}\frac{\partial}{\partial\rho}\right) + \frac{\hbar^2}{2m}\left(\frac{l}{\rho}\right)^2 + \frac{\sigma l}{2}\hbar\omega_c + \frac{m}{8}(\omega_c\rho)^2 + V(\rho)\right] R(\rho) = ER(\rho). \quad (2)$$

Here $\omega_c = |e|\ B/(mc)$ is the cyclotron frequency and, as anticipated above, the ring-like confinement is assumed to be described by the radial potential,

$$V(\rho) = \begin{cases} 0, & \rho \le \rho_1 \\ -V_0, & \rho_1 \le \rho \le \rho_2 \\ 0, & \rho \ge \rho_2 \end{cases} \quad (3)$$

where ρ_1 (ρ_2) is the inner (outer) radius of the quantum ring and $V_0 \ge 0$. Here and below, to specify the electron ("e") and hole ("h") parameters, we replace: $m \to m_{e,h}$, $\sigma \to \sigma^{e,h}$ (with $\sigma^e = -1$, $\sigma^h = +1$), $R \to R^{e,h}$, $E \to E^{e,h}$, $l \to l^{e,h}$, $V(\rho) \to V^{e,h}(\rho)$, $V_0 \to V_0^{e,h}$, $\omega_c \to \omega_c^{e,h}$.

As it is known [36], the radial solution to equation (2) is expressed in terms of the confluent hypergeometric functions $M(a,b,z)$ and $U(a,b,z)$ [37]. Their (third) argument, the dimensionless variable $z = \frac{\rho^2}{2l_m^2}$, is the magnetic flux through the disk of radius ρ in units of the elementary magnetic flux. The magnetic length scale $l_m = \sqrt{\frac{\hbar c}{|e|\ B}}$ is the natural length to measure the magnetic field dependence of the QR with different radii.

The energy spectrum of the particle can be written in a form similar to the Landau levels expression [36]:

$$E_{\nu,l} = \hbar\omega_c\left(\nu + \frac{\sigma l + |l| + 1}{2}\right) = \hbar\omega_c\left(n_L + \frac{1}{2}\right), \quad (4)$$

where n_L is the principal quantum number. We count the energy from the bottom of the potential well. The lowest subband of energy $\hbar\omega_c^{e,h}\left(\nu^{e,h} + \frac{1}{2}\right)$ corresponds to strictly non-positive (non-negative) values of the magnetic quantum numbers l^e (l^h). Although for a free charge n_L is an integer, for a restricted motion in the plane the radial quantum numbers ν (and therefore, n_L) become non-integer, and depend on the angular momentum quantum numbers l, by virtue of the boundary conditions.

In order to determine the eigenenergies one must impose that the radial eigenfunction $R(\rho)$ satisfies the continuity conditions at the interior and exterior QR boundaries, i.e. in the limits $\rho \to \rho_1$ and $\rho \to \rho_2$. The boundary conditions lead to a homogeneous system of linear equations for the integration constants. By making use of the determinant properties, we arrive at the following form of the secular equation for the allowed single particle energy eigenvalues:

see equation (5) above

Here $b = 1 + |l|$, $r_{1,2} = \rho_{1,2}/l_m$, the primes denote derivatives on the radial coordinate, and

$$\nu_{ex} = \nu - \delta = \nu - \frac{\hbar\omega_c}{V_0}. \quad (6)$$

The quantum numbers ν and ν_{ex} characterize the motion interior and exterior of a ring of width $W = \rho_2 - \rho_1$. The roots ν of the secular equation (5) are calculated numerically for each value of $|l|$, and the corresponding energy eigenvalues are obtained from (4).

An important observation is that the secular equation depends on the particle parameters only through the ratio $\hbar\omega_c/V_0$. Therefore, the solutions of the secular equation and, thus, the wave functions are exactly the same for electrons and holes if the following relationship between the potential and masses is fulfilled:

$$V_0^h\ m_h = V_0^e\ m_e. \quad (7)$$

The importance of the above equality lies in the fact that one may consider equation (7) as the condition for the absence of e–h radial polarization. Otherwise, when equation (7) is not obeyed, the eigenenergies and eigenfunctions for the electron and hole are different and radial polarization occurs.

3 Numerical results for energy spectra in QRs

The energy spectra have been studied systematically as a function of magnetic field in nanorings of varying geometry. We have calculated the energy spectra for both electron and hole in QRs with various confinement potentials in the range $V_0^e = 50$–500 meV, $V_0^h = 17$–170 meV, respectively. We show only the results for the case $V_0^e = 50$ meV, $V_0^h = 17$ meV because the dependence of period of the ground state A-B oscillations on magnetic field has been found very much the same for both small and large

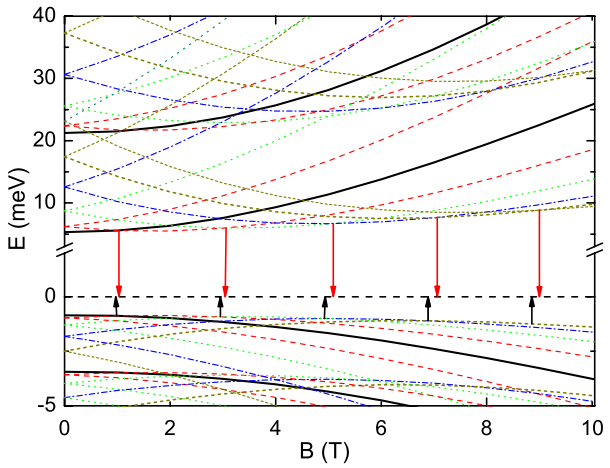

Fig. 1. Electron and hole energy levels versus applied magnetic field in a potential well of $\rho_1 = 15$ nm, $\rho_2 = 40$ nm, $V_0^e = 50$ meV, and $V_0^h = V_0^e/3 = 17$ meV. The intervals for existence of dark e–h pair are delimited by the nearest arrows.

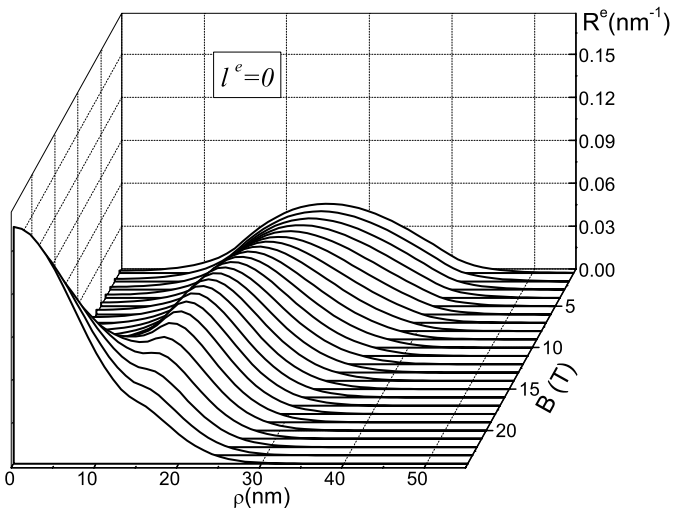

Fig. 2. The evolution of the radial eigenfunction for the singlet electron, $l^e = 0$, with increasing magnetic field in a ring with the same parameters as in Figure 1.

confinement energies. For definiteness, the quantum ring is assumed to be made of GaAs material embedded in AlGaAs, and the effective masses are accordingly taken to be $m_e = 0.0667\ m_0$, $m_h = 0.5\ m_0$, m_0 being the free electron mass.

In Figure 1 we show the dependence of the electron and hole energy as a function of magnetic field for several quantum numbers l. We plot the calculated energy levels versus magnetic field for positive and negative l states (whose energies converge to each other as the magnetic field goes to zero). From the energy level dependence with the magnetic field (see Fig. 1), we can observe how the angular momentum quantum number corresponding to the lowest energy state varies with increasing field. The intersections of the lowest energy levels indicate transitions with $|\Delta l| = 1$ at some specific values of the magnetic field, marked by arrows in Figure 1; hence the ground state energy curve consists of arch pieces crossing at these values.

At this point, we would like to note that, since for the electron in GaAs quantum dots the value of the g factor is equal to 0.17 [38], the spin splitting energy value ($g\mu_B B$, where μ_B is the Bohr's magneton) is of 0.24 meV at $B = 25$ T. Thus it looks reasonable to neglect, in the first approximation, the difference in the energy between the spin up and down states. The Zeeman gap energy was also found to be negligibly small for magnetoexcitons in unstrained GaAs/AlxGa$(1-x)$As [32].

The above nearly periodic dependence of the energy on magnetic flux, $\Phi = \pi\ \rho^2 B$, through the average area of a thin annulus is a manifestation of the A-B effect [1]. Indeed, the energy of a charged particle with mass m in a 1D ring of radius ρ is

$$E = \frac{\hbar^2}{2m\rho^2}\left(|l| - \frac{\Phi}{\Phi_0}\right)^2, \tag{8}$$

where $\Phi_0 = 2\pi\hbar c/|e|$ is the elementary magnetic flux quantum. Furthermore, the effect of the penetration of magnetic field into the ring itself reveals in a non parabolicity of the energy levels, as shown in Figure 1, and in the condensation of the ground state energy to the Landau level at high fields [39].

Once the eigenvalue problem has been solved, the explicit eigenfunctions obeying the boundary conditions can also be calculated. Figure 2 shows the radial eigenfunction for the singlet electron state, $l^e = 0$, as magnetic field increases. Figure 2 also illustrates that, when magnetic field increases from zero, the maximum of R^e evolves from inside of the QR to the center of the ring. In the low field region, the wave function is nearly symmetric (peaked at the average radius of the ring), while for high fields, the maximum of R^e is peaked at $\rho = 0$ and warped near the inner boundary in the high field region. With increasing magnetic field the probability of finding the singlet electron moves from the confinement region to the QR center through the inner barrier, whereas the ground state (not shown) associated with some $l^e \neq 0$ localizes away from the QR edges, and approaches to the energy of the Landau level.

In Figure 1 the magnetic field values corresponding to the successive changes of l (marked by arrows) depend on the effective mass and height of the confinement potential and thus they are different for the electron and hole if equation (7) is not fulfilled. Figure 1 suggests that there exist a quite narrow but finite ranges of magnetic field values where the total angular momentum of the e–h pair, $L_z = l^e + l^h$, changes abruptly from $L_z = 0$ to a non vanishing value. This has an impact on the oscillator strength of the e–h pair. Indeed, the photoluminescence intensity

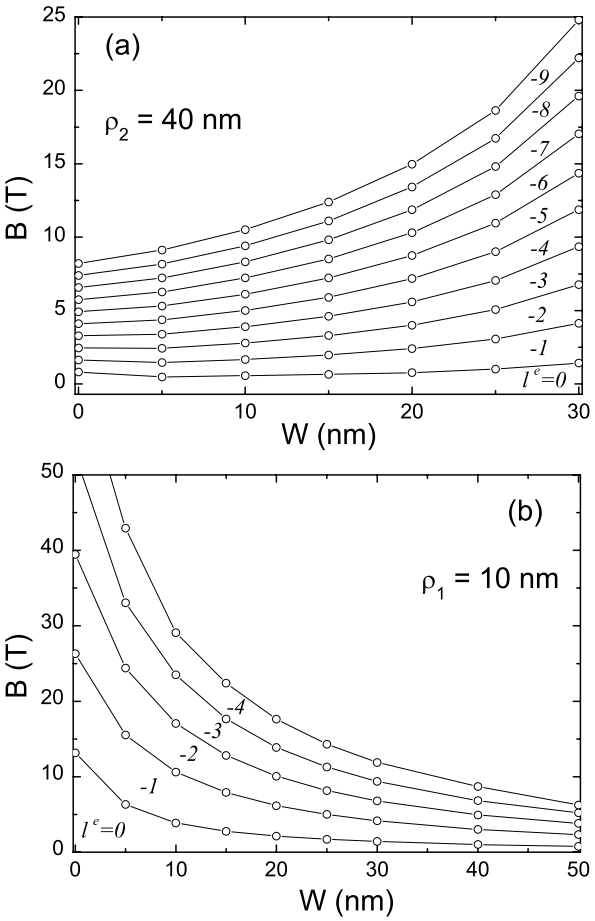

Fig. 3. Phase diagrams showing the electron angular momentum transitions, $l^e \to l^e - 1$, in a QR of the $V_0^e = 50$ meV, for fixed outer radius ρ_2=40 nm (a), and fixed inner radius $\rho_1 = 10$ nm (b).

is proportional to the square of the overlap integral

$$\int \Psi_e(\rho,\varphi)\Psi_h(\rho,\varphi)d\boldsymbol{r} = \Xi\ \delta_{0,L_z},$$

$$\Xi = \int_0^\infty R_{\nu^e,l^e}(\rho)R_{\nu^h,l^h}(\rho)\rho d\rho. \quad (9)$$

It follows from equation (9) that the optical emission process must obey the selection rule $L_z = 0$, i.e. the exciton emission is only possible for the singlet state of the e–h pair in which $l^e = -l^h$ [15]. Thus, the electron-hole recombination is forbidden within the intervals where the so-called dark exciton ($L_z \neq 0$) becomes the ground state. These intervals correspond to the domains between nearest arrows in Figure 1. Since the overlap integral Ξ has a very weak dependence on B (as obtained from our numerical calculations), these are the only domains where e–h recombination is forbidden. In the particular case of a QR with infinite barriers, equation (7) holds trivially, and the photon can be emitted for any value of B.

Figures 3a and 3b summarize our numerical results concerning the angular momentum transitions in the form of phase diagrams of magnetic field versus ring width [28]. In both figures, the flux of the magnetic field must approach an integer number of the elementary flux for the 1D case ($W \to 0$), in accordance to the well known expression (8).

For fixed ρ_2, the magnetic field period of angular momentum transitions increases with the increasing width of the QR, as illustrated in Figure 3a. As ρ_1 vanishes, i.e. $W \to \rho_2$ the period of A-B oscillations increases asymptotically to infinity. The change in topology of the confining potential results in the disappearance of the angular momentum transitions in the case of a quantum disk. On the other hand, as Figure 3b shows, for a fixed ρ_1, as the width increases the magnetic field period decreases monotonically. In the large width limit, the A-B flux tends asymptotically to the characteristic periods of a quantum antidot system, see for example [29].

Surprisingly, our calculations (not shown here) indicate that the period of A-B oscillations in a magnetic field is almost not affected by a tenfold increase of the confining potential. This was verified for various radii ρ_1, ρ_2, but keeping the fixed ratio $V_0^e/V_0^h = 3$, for both electron and hole. In either potential the phase diagrams are nearly indiscernible due to the fact that the scaling equation (7) is approximately satisfied. The magnitude of the potential influences, for instance, the range of magnetic field for which the bound ground state transforms into an unbound and vice versa (see below).

Notice that the ultimate reason for the disappearance of the photoluminescence signal from a ring is the selection rules following from the conservation of the total angular momentum of the e–h pair. Therefore, it is tempting to speculate that our results on the periodicity of the disappearance of the optical signal with the magnetic field, as based on the rotational symmetry of the 2D system, remain valid, at least qualitatively, in the presence of an e–h Coulomb interaction. As it was shown in [40,41], for a system of interacting electrons the magnetization is nearly the same as for the non-interacting electrons due to conservation of angular momentum in the 2D quantum rings. The numerical results of [41] demonstrate that, in the lowest Landau level, the electron-electron Coulomb interaction shifts the non-interacting energy spectrum to higher energies. Although it is commonly believed that the A-B effect exists also for excitons, in the weakly interacting regime the very recent studies show some discrepancy on this issue [26,27]. In this regime strong A-B oscillations with the magnetic field remain [26] (also our approach supports this statement). In the weakly interacting regime, in the first order of perturbation theory, the electron-hole Coulomb interaction shifts rigidly by a negative constant the non-interacting energy spectrum to lower energies [27]. The natural continuation of the present research is the investigation of the effect of the e–h interaction on the magneto-optical transitions by complete diagonalization of the Hamiltonian, see e.g. [41], using our electron hole non-interacting basis. This might appear to be useful as complementary to the other approaches [21,26] being under intensive investigations now. In the strongly correlated

regime, the only remaining A-B effect manifests itself in oscillating excited states [26,27]. A more complete study of effects of the Coulomb interaction for polarized e–h pair in continuous 2D model of QRs beyond perturbation theory is still to be done.

As examples of possible qualitative effects coming from the turning on an interaction, we refer also on exact non-perturbative results obtained for discrete-lattice rings, which in contrary to a Galilean-invariant system, see e.g. [40,42], yield such dependence of the magnetization on the correlation. It was shown that, as the interaction strength varies, the ground state gaps open and close, see for example [42], while only for gapless excitations, the amplitude of the A-B oscillation is not exponentially small [23]. In the Hubbard chain, the strong correlation results in the changes of magnitude and period of the ground state energy oscillations, see e.g. [43]; the period of the A-B oscillations, depending on magnetization of 1D ring of the fermion system with attraction, alters from integer to half integer of Φ_0 [23]. The extra frequencies to the fundamental Aharonov-Bohm frequency of the exciton oscillations were shown to appear in a ring described by the attractive Hubbard model on the coupled concentric 2D annular lattices [21]. In our paper we assume that the QR is an ideal 2D ring and that the roughness of boundary shape nor defects do not smash periodicity of equilibrium thermodynamic quantities [6]. It has been shown that elastic scattering does not attenuate the A-B effect in a ring with disorder [5].

4 Curvature effect on tunneling through ring under a magnetic field

In this section we will supplement our quantum mechanical calculations by a semi-classical determination of the magnetic field values $B_1(B_2)$ for which the electron or hole states cross the inner (outer) ring boundaries in connection to the feasible domain for the existence of dark excitons.

The radial polarization of carriers with different masses in a finite confining potential is essentially a quantum mechanical effect. It appears due to the fact that the probability of tunneling through a potential barrier for one charged particle exceeds the probability for the other.

The semi-classical WKB theory says that the quantum energies for 2D motion of a charged particle in a cylindrically symmetrical potential and under a magnetic field are defined by the roots of the equation [36]

$$\pi\ (\nu+\gamma) = \sum_i \int_{\hat{r}_i}^{\hat{r}_{i+1}} \sqrt{\frac{E}{\hbar\omega_c} - U_{\mathit{eff}}(l,r,\delta)}\ dr\,, \qquad (10)$$

where γ is a constant and the integral is over the classically allowed region (where the square root has a positive argument) limited by a couple of turning points $(\hat{r}_i, \hat{r}_{i+1})$. To define this region we consider the minima of the effective potential $U_{\mathit{eff}}(l,r,\delta)$ at a given magnetic field.

In our case, the effective potential is defined by the finite confinement potential, which takes zero values outside the QR, equation (3), combined with the quantum-mechanical centrifugal potential barrier l^2/r^2, and with the magnetic potential $r^2/4-\sigma l$:

$$U_{\mathit{eff}}(l,r,\delta) = \begin{cases} (-\sigma l/r + r/2)^2, & r \le r_1, \\ -2/\delta + (-\sigma l/r + r/2)^2, & r_1 \le r \le r_2 \\ (-\sigma l/r + r/2)^2, & r \ge r_2\,, \end{cases} \qquad (11)$$

where $r=\rho/l_m$, r_1 can be considered as the inner radius of the ring or antidot, r_2 as the outer radius of ring or disk in units of magnetic length, and $1/\delta$ is the number of Landau levels inside the potential, equation (6).

We shall substitute $\nu \to \nu^{e,h}$, $\delta \to \delta^{e,h}$, $m \to m_{e,h}$, $E \to E^{e,h}$, $V_0 \to V_0^{e,h}$, $l \to l^{e,h}$, $\sigma = \mp 1$, when discussing the electron and the hole, respectively. The effective potential depends on the absolute value of the magnetic quantum number $\sigma l = |l|$ for the electron as well as for the hole in the ground state. The integration allows us to obtain the transcendental equation for the energy as explained in Appendix A.

At high magnetic field, the appearance of the bulk states with Landau energy in the QR (Landau condensation) [39] results in a factorization of the secular equation into the characteristic equation for the antidot of radius ρ_1 and that for the circular disk of radius ρ_2 [44]. That allows us to consider separately the states of a charged particle near the outer and inner boundaries of ring confining potential.

Firstly, we shall consider negative (positive) l states of the electron (hole) in a circular disk confining potential. The effective potential derivative vanishes at $r_l = \sqrt{2|l|}$, where the probability of finding the charge in the eigenstate $\Psi_{\nu,l}$ has its maximum. If $r_l < r_2$, there is one well effective potential with the minimum value $U_{\mathit{eff}}(l,r_l,\delta) = -2/\delta$ at $r=r_l$. If $|l|$ is sufficiently large, the probability of finding a charged particle out of the confinement region, $r_l > r_2$ appears to be finite. Therefore, there emerges a double well effective potential for the states because of the appearance of two minima: the inside minimum is just at the outer boundary, $r-r_2 \to 0^-$ (because of the step-like change of the confinement potential) and the outside minimum is at $r_l > r_2$. We define the magnetic quantum number l_2^* as the number such that for $|l| \le l_2^*$ the minimum of U_{eff} in the QR, at $r-r_2 \to 0^-$, is deeper than the minimum out it, at $r=r_l$. These minima become nearly equal when the angular momentum quantum number reaches the value l_2^* (up to its modulus)

$$U_{\mathit{eff}}(l_2^*, r_2, \delta) \approx U_{\mathit{eff}}(l_2^*,\ r_l, \delta), \qquad r_l > r_2$$

$$l_2^* = \left[\frac{\Phi_2}{\Phi_0} + \sqrt{2\frac{\rho_2^2}{\hbar^2}V_0 m}\right]. \qquad (12)$$

In equation (12) Φ_2 is the magnetic flux threading the disk of radius ρ_2, and the square brackets denote the integer part of the wrapped expression. From equation (12) we

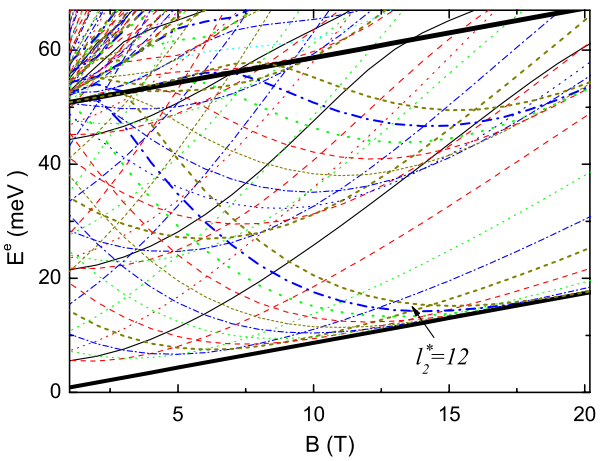

Fig. 4. The calculated electron energy levels as a function of magnetic field for a QR of $\rho_1 = 15$ nm, $\rho_2 = 40$ nm, and $V_0^e = 50$ meV. The solid line corresponds to $l = 0$, dashed lines to $|l| = 1, 5, 9$, dotted lines to $|l| = 2, 6, 10$, dash-dotted lines to $|l| = 3, 7, 11$, short-dotted lines to $|l| = 4, 8, 12$. The two straight parallel thick lines depict the lowest Landau levels inside ($E_{0,0}^e$) and outside ($E_{0,0}^e + V_0^e$) the QR confinement.

estimate l_2^* ($B = 1\ T$) to be about 12 for the electron in the potential $V_0 = 50$ meV. Indeed, the curve for the energy of the electron state with $l^e = 10$ starts to split from the Landau level outside the ring ($E_{0,0}^e + V_0^e$) in a low magnetic field, as Figure 4 shows. Therefore, the energy level for $|l| \geq l_2^*$, manifests an inflection, and then approaches the Landau level inside the QR ($E_{0,0}^e$) at high magnetic fields. An increasing magnetic field pushes negative eigenstates for the electron to the origin, as it is shown in Figure 2. As it follows from equation (12), the maximum of probability density of the state associated with a given l localizes inside of the external QR boundary when $B \geq B_2$:

$$B_2(l) = -\frac{c\sqrt{8\ m\ V_o}}{|e|\rho_2} + |l|\frac{\Phi_0}{\pi\rho_2^2}. \tag{13}$$

The S-state ($l = 0$) has the global minimum of the effective potential fixed at the center of the disk at arbitrary magnetic field. In the case of disk geometry, only this state contributes appreciably to the ground state for low fields, whereas the energies of the nonzero angular momentum states just merge successively into the Landau level of the $l = 0$ state in high magnetic field [39]. In the case of annular geometry, with increasing magnetic field the states consecutively tunnel via the inner barrier and, due to its contribution, the magnetic quantum number $|l|$ of the ground state increases starting from zero.

Secondly, we address the problem of inward tunneling of the l states in the antidot confining potential. There is a double well for the S-state and the probability density has two maxima binding to the minima of the effective potential. In a weak magnetic field the local minimum at $\rho = 0$ is higher than the step-wise minimum at the inner boundary of the ring, $\rho - \rho_1 \to 0^+$. Under a certain magnetic field, $B_1(l = 0)$, when the confinement barrier becomes equal to the characteristic magnetic energy, $V_0 = \frac{1}{8}m\omega_c^2\rho_1^2$, the S-state penetrates into the ring opening, as Figure 2 shows. In the case of arbitrary l, the two wells of effective potential level at the threshold value of magnetic field

$$B_1(l) = \frac{c\sqrt{8mV_0}}{|e|\rho_1} + |l|\frac{\Phi_0}{\pi\rho_1^2}, \tag{14}$$

and the l state appears in the ring opening if $B \geq B_1(l)$. From equation (14) we estimate $B_1^e(l^e = 0) = 25.94$ T that correlates well with the $E(B)$ dependence shown in Figure 5a. So far, our semi-classical estimates of B_1 and B_2 (or l_2^*) are in good agreement with the results of quantum mechanical calculations. Taking together the conditions for passage through the inner and outer barriers, we conclude that the l state is trapped inside the ring if $B_2(l) \leq B \leq B_1(l)$. We present in Appendix A the transcendental equations for the energy of the l state within this range of the magnetic field values.

The energy is a function of $\rho_l = l_m\sqrt{2|l|}$, which is the guiding cyclotron orbit center for unrestricted motion in a plane [45]. States with ρ_l in the vicinity of the boundaries of a confining potential are known as *edge states*. The distance from the orbit center of an edge state to the boundary is less than the magnetic length. There are *inner* and *outer* edge states oppositely circulating from the inside of the QR of the infinite potential under a weak magnetic field, which induce diamagnetic and paramagnetic moments, respectively [46]. The inflection of the energy curves shown in Figures 4 and 5a can be related to the edge states of the electron and interpreted in terms of the magnetic susceptibility. Indeed, the magnetization and the magnetic susceptibility of the $R_{\nu,l}$ state of a single-charged particle are defined by

$$M_{\nu,l}(B) = -\frac{\partial}{\partial B}E_{\nu,l}(B), \tag{15}$$

$$\chi_{\nu,l} = \frac{\partial}{\partial B}M_{\nu,l}(B). \tag{16}$$

The magnetic susceptibility of the l state, $\chi_{\nu,l}$ changes sign at an inflection point of the curve $E_{\nu,l}(B)$. We have found, as Figure 4 shows, that the energy of an eigenstate with a given l, beginning from $|l| = l_2^*$ reveals an inflection due to the change in $M_{\nu,l}(B)$ on the outer boundary. The electron edge state associated with $|l| \geq l_2^*$ circulates in counter clockwise direction (about the z axis) nearby the external boundary from outside. With increasing magnetic field the center of the wave function approaches the ring origin and the circulation changes direction to the opposite one inside of the external boundary due to the scattering from it. Then, as the magnetic field increases, this eigenstate of positive energy beyond ρ_2, transforms into the ground state, $-|V_0| \leq E \leq 0$, in an interior region of the QR. Figure 4 shows this type of inflection point on the energy level ($M_{\nu,l}(B) > 0$) for the electron. As the magnetic field increases, the energy curve is flattened nearby the Landau level. Finally, it tends asymptotically to the bulk level in the interior region of the ring opening as Figure 5a shows. As a result, the electron edge state circulates in clockwise

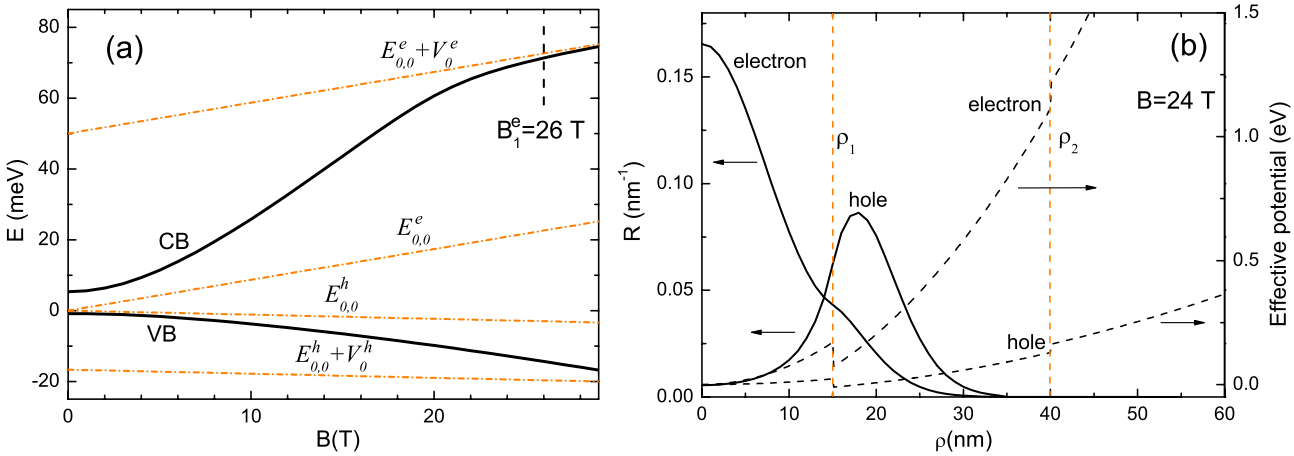

Fig. 5. (a) The calculated ground state electron and hole energies versus magnetic field for the QR of $\rho_1 = 15$ nm, $\rho_2 = 40$ nm, and $V_0^e = 50$ meV, $V_0^h = 17$ meV, respectively. (b) Corresponding electron and hole radial wave functions at a magnetic field of $B = 24$ T, in the same QR. The figure also shows the electron and hole potentials (right scale).

direction along the inner boundary from inside. The inflection of the raising energy curve $E(B)$ shown in Figure 5a, implies the change of the magnetic response from diamagnetic, $\chi_{\nu,l} \leq 0$, to paramagnetic, $\chi_{\nu,l} \geq 0$, whereas the inflection of the falling energy curve indicates the inverse change on the outer boundary, see Figure 4.

The energy branch for the singlet state of the hole is also depicted in Figure 5a. The maximum of the electron wave function is at the center of the QR. The shoulder (a second maximum at lower fields [see Fig. 2]) at $\rho = 15$ nm is due to a deep in the electron potential, as shown in Figure 5b. The hole wave function exposes only one peak located at the absolute potential minimum, because $B \leq B_1^h(l^h = 0)$, where $B_1^h(l^h = 0) = 41$ T.

For the singlet pair $L_z = l^e + l^h = 0$ we readily derive from equations (13, 14) the difference between the magnetic field values for the the electron and the hole states when crossing the outer and inner boundaries of the confining potential region

$$B_2^e - B_2^h = +\frac{c\sqrt{8\ m_h\ V_0^h}}{|e|\rho_2}(1-\Gamma), \tag{17}$$

$$B_1^e - B_1^h = -\frac{c\sqrt{8\ m_h\ V_0^h}}{|e|\rho_1}(1-\Gamma), \tag{18}$$

where

$$\Gamma = \sqrt{\frac{m_e\ V_0^e}{m_h\ V_0^h}}. \tag{19}$$

The + (−) sign and the index 2 (1) stand for outer (inner) boundary. We employ a value of potential depth for the hole of approximately one third of the electron one. We estimate $\Gamma \approx 0.63$ with these data, and conclude from equation (17) that, for the $L_z = 0$ pair at arbitrary l, the electron state becomes bound at a magnetic field B_2^e which is greater that of the hole, $B_2^e \geq B_2^h$. In contrast, the electron state becomes unbound in the QR opening at a magnetic field value B_1^e lower than the one for the hole, $B_1^{(e)} \leq B_1^{(h)}$. The electron passes through the barriers at the same magnetic field as the hole if $\Gamma = 1$, in agreement with the implicit condition of the absence of radial polarization, equation (7).

If we are interested in the magnetic field values where the PL disappears since total angular momentum of magneto-exciton is not zero, it follows from the quantum mechanical calculations that these intervals are rather narrow for the selected parameters. Perhaps due to this, the A-B effect has not yet been observed in optical experiments in type I semiconductor structures. Nevertheless, from equations (17) and (18) one might conclude that the domain for disappearance of the PL signal depends on inherent and geometric parameters of self-assembled QR. Our proposal is to extend the interval for existence of dark exciton in magnetic fields by choosing semiconductors with parameter Γ as smaller as possible to increase polarization and to allow the optical observation of the neutral exciton A-B effect.

5 Conclusions

We have explored in detail the role of the finite width effects and potential depth on the dispersion of energy levels of a QR as a function of magnetic field and angular momentum quantum number. The results of the numerical calculations have been summarized in phase diagrams for the angular momentum transitions as a function of magnetic field and various geometry parameters. We have studied the transitions between the unbound states and the ground state through the energy spectra, and proposed formulae to estimate the magnetic field values related to these transitions. That gives rise to a suggestion for detection of A-B optical signal from the electron-hole pair confined in the semiconductor quantum ring, perpendicular to magnetic field. Taking into account the Coulomb interaction by the complete diagonalization of the exciton Hamiltonian is the problem for future study.

This work has been supported by the grant No. $-SAB2000-0353$ from the Ministry of Education, Science, Culture and Sport of Spain. One of the authors, T.B., would like to thank José A. de Azcárraga for valuable comments on the manuscript.

Appendix A: Finite width corrections

The Bohr-Sommerfield quantization rule determining the allowed energies of the particle in the effective potential, equation (10), on substituting $z = r^2/2$, takes the form

$$2\ \pi\ (\nu+\gamma) = \sum_i \int_{\hat{n}_i}^{\hat{n}_{i+1}} \lambda(z)\ \frac{dz}{z}, \tag{A.1}$$

where $z_1 \le \hat{n}_i$, $\hat{n}_{i+1} \le z_2$, and

$$\lambda(z) \equiv \lambda(z; z_1, z_2) = \sqrt{(z-z_1)(z_2-z)}. \tag{A.2}$$

Here the integration range is split into two intervals for the two-well effective potential for the energy between its two minima values, whereas there is one interval for the one-well potential.

Evaluating the integral yields

$$\begin{aligned}\kappa(z; z_1, z_2) &= \int \lambda(z; z_1, z_2)\ \frac{dz}{z} \\ &= \lambda(z) - \bar{z} \arctan \frac{\bar{z}-z}{\lambda(z)} \\ &\quad + \sqrt{z_1\ z_2} \arctan \frac{z_1\ z_2 - \bar{z}\ z}{\lambda(z)}. \end{aligned} \tag{A.3}$$

We refer to the electron throughout this Appendix, and introduce the dimensionless energy variable $\epsilon = 2\ \frac{E}{\hbar\omega_c}$, so that

$$z_1\ z_2 = l^2, \qquad \bar{z} = \frac{1}{2}(z_1+z_2) = \epsilon - l\ . \tag{A.4}$$

We consider further the states bound to the lowest minimum inside the confining potential within the range, $B_2(l) \le B \le B_1(l)$. The limits of integration are $\hat{n}_1 = N_1$, $\hat{n}_2 = N_2$, where $N_{1,2} = \Phi_{1,2}/\Phi_0$ is the number of magnetic fluxes through a circular disk of radius $\rho_{1,2}$, respectively. In the limiting case of a narrow ring, $W = \rho_2 - \rho_1 \ll l_m$, we obtain equation (8) for the energy spectrum of the particle in the zero-th order approximation on $W/\rho_1 \ll 1$, and the results of [47] in the next order. In the case of a wide ring, $W \gg l_m$, when the left and right turning points are $\hat{n}_1 = z_1$, $\hat{n}_2 = z_2$, and, $\gamma = 1/2$, we recover the bulk Landau energies equation (4).

At fixed high magnetic field the bulk Landau states have the inner and outer edge states from both sides of the QR boundary. For the edge states, the spectra can be re-written in the form which is characteristic of the 2D oscillator

$$E_{\nu,l} = 2\ \hbar\ \omega_c \left(\nu + \frac{l+|l|}{4} + \frac{1}{2}\right) + f_{\nu,l}.$$

At high magnetic field, for the inner edge states characteristic of the antidot, the integration is over the interval $[N_1, z_2](N_1 \ge z_1)$ and from equation (A.1) we arrive at:

$$\begin{aligned}2\ \pi\ (\nu+\gamma) &= -\lambda(N_1) + \frac{\pi}{2}(\epsilon - l - |l|) \\ &\quad + (\epsilon - l) \arctan \frac{\epsilon - l - N_1}{\lambda(N_1)} - |l| \arctan \frac{l^2 - (\epsilon - l)\ N_1}{\lambda(N_1)}, \end{aligned} \tag{A.5}$$

where λ is defined by (A.2) with $z_{1,2}$ from (A.4),

$$\lambda(N_1) = \sqrt{-N_1^2 + 2(\epsilon - l)N_1 - l^2}\,.$$

Then, for this case $f_{\nu,l}$ is given by

$$\begin{aligned}f_{\nu,l}^{AD} = \frac{\hbar\ \omega_c}{\pi} \Bigg[&\lambda(N_1) - (\epsilon - l) \arctan \frac{\epsilon - l - N_1}{\lambda(N_1)} \\ &+ |l| \arctan \frac{l^2 - (\epsilon - l)\ N_1}{\lambda(N_1)} \Bigg]. \end{aligned} \tag{A.6}$$

It turns out, from equation (A.6), that the inner perimeter correction to the magnetization is a diamagnetic one, i.e. $-\frac{\partial}{\partial B} f_{\nu,l}^{AD}(B) \le 0$.

For the outer edge states peculiar to the disk geometry, the integration is over the interval $[z_1, N_2](N_2 \le z_2)$ and $f_{\nu,l}$ is

$$\begin{aligned}f_{\nu,l}^{D} = \frac{\hbar\ \omega_c}{\pi} \Bigg[&-\lambda(N_2) + (\epsilon - l) \arctan \frac{\epsilon - l - N_2}{\lambda(N_2)} \\ &- |l| \arctan \frac{l^2 - (\epsilon - l)\ N_2}{\lambda(N_2)} \Bigg]. \end{aligned} \tag{A.7}$$

The outer perimeter correction to the magnetization proves to be a paramagnetic one, $-\frac{\partial}{\partial B} f_{\nu,l}^{D}(B) \ge 0$, while the inner perimeter correction is diamagnetic one.

The correction to the energy from the inner, $f_{\nu,l}^{AD}$, and outer, $f_{\nu,l}^{D}$, boundaries of the ring are of opposite sign (diamagnetic and paramagnetic shift of the Landau state), though, overall, the surface states increase the bulk Landau energy, since that is a universal feature of an enclosure [48].

The intersections of the set of ascending energy levels for the inner edge states, equation (A.6), with the set of descending energy levels for the outer edge states, equation (A.7), allow to determine the magnetic field values for angular momentum transitions where the energy is degenerate.

References

1. Y. Aharonov, D. Bohm, Phys. Rev. **115**, 485 (1959)
2. L. Lévy, G. Dolan, J. Duinsmuir, H. Bouchiat, Phys. Rev. Lett. **64**, 2074 (1990)
3. D. Mailly, C. Chapelier, A. Benoit, Phys. Rev. Lett. **70**, 2020 (1991)
4. A. Fuhrer, S. Lüscher, T. Ihn, T. Heinzel, K. Ensslin, W. Wegscheider, M. Bichler, Nature **413**, 822 (2001)

5. M. Büttiker, Y. Imry, R. Landauer, Phys. Lett. A **96**, 365 (1983)
6. N. Byers, C.N. Yang, Phys. Rev. Lett. **7**, 46 (1961)
7. Y. Gefen, Y. Imry, M.Ya. Azbel, Phys. Rev. Lett. **52**, 129 (1984)
8. V. Halonen, T. Chakraborty, P. Pietiläinen, Phys. Rev. B **45**, 5980 (1992)
9. A.V. Chaplik, JETP Lett. **62**, 900 (1995)
10. R.A. Römer, M.E. Raikh, Phys. Rev. B **62**, 7045 (2000)
11. M. Bayer, M. Korkusinski, P. Hawrylak, T. Gutbrod, M. Michel, A. Forchel, Phys. Rev. Lett. **90**, 186801 (2003)
12. E. Ribeiro, A.O. Govorov, W. Carvalho, G. Medeiros-Ribeiro, Phys. Rev. Lett. **92**, 126402 (2004)
13. C. Shulhauser, R.J. Warburton, A. Högele, A.O. Govorov, K. Karrai, J.M. Garcia, B.D. Gerardot, P.M. Petroff, Physica E **21**, 184 (2004)
14. A. Lorke, R.G. Luyken, A.O. Govorov, J.P. Kotthaus, J.M. Garcia, P.M. Petroff, Phys. Rev. Lett. **84**, 2223 (2000)
15. A.V. Kalameitsev, V.M. Kovalev, A.O. Govorov, JETP Lett. **68**, 669 (1998)
16. A.O. Govorov, S.E. Ulloa, K. Karrai, R.J. Warburton, Phys. Rev. B **66**, 081309 (2002)
17. S.E. Ulloa, A.O. Govorov, A.V. Kalameitsev, R.J. Warburton, K. Karrai, Physica E **12**, 790 (2002)
18. A.O. Govorov, A.V. Kalameitsev, R.J. Warburton, K. Karrai, S.E. Ulloa, Physica E **13**, 297 (2002)
19. J. Song, S.E. Ulloa, Phys. Rev. B **63**, 125302 (2001)
20. H. Hu, J.L. Zhu, D.J. Li, J.J. Xiong, Phys. Rev. B **63**, 195307 (2001)
21. F. Palmero, J. Dorgnac, J.C. Eilbeck, R.A. Römer, Phys. Rev. B **72**, 075343 (2005)
22. Y. Aharonov, A. Casher, Phys. Rev. Lett. **53**, 319 (1984)
23. A.A. Zvyagin, JETP **76**, 167 (1993)
24. A.A. Zvyagin, T.V. Bandos, JETP **82**, 135 (1996)
25. A.V. Maslov, D.S. Citrin, Phys. Rev. B **67**, 121304 (2003)
26. L.G.G. V. Dias da Silva, S.E. Ulloa, T.V. Shahbazyan, Phys. Rev. B **72**, 125327 (2005)
27. Z. Barticevic, M. Pacheco, J. Simonin, C.R. Proetto, Phys. Rev. B **73**, 165311 (2006)
28. K.L. Janssens, B. Partoens, F.M. Peeters, Phys. Rev. B **64**, 155324 (2001)
29. K.L. Janssens, B. Partoens, F.M. Peeters, Phys. Rev. B **66**, 075314 (2002)
30. D. Haft, C. Shulhauster, A.O. Govorov, R.J. Warburton, K. Karrai, J.M. Garcia, W. Schoenfeld, P.M. Petroff, Physica E **13**, 165 (2002)
31. A. Rastrelli, S. Stufler, R. Songmuang, C. Manzano, G. Costantini, K. Kern, A. Zrenner, D. Bimberg, O.G.Schmidt, Phys. Rev. Lett. **92**, 166104 (2004)
32. Y. Sidor, B. Partoens, F.M. Peeters, N. Shildermans, M. Hayne, V.V. Moshchalkov, A. Rastrelli, O.G. Schmidt, Phys. Rev. B **73**, 155334 (2006)
33. K. Maschke, T. Meier, P. Thomas, S.W. Koch, Eur. Phys. J. B **19**, 599 (2001)
34. W.C. Tan, J.C. Inkson, Phys. Rev. B **53**, 6947 (1995)
35. V. Fock, Z. Phys. **47**, 446 (1928)
36. L. Landau, E. Lifschitz, *Quantum mechanics* (Mir, Moscow, 1996)
37. M. Abramowitz, I.A. Stegun, *Handbook of Mathematical Functions*, Natl. Bur. Stand. Appl. Math. Ser. No. **55**, (U.S. GPO, Washington, D.C.,1970)
38. K. Nishibayashi, T. Okuno, Y. Masumoto, H.-W. Ren, Phys. Rev. B **68**, 035333 (2003)
39. M. Robnik, J. Phys. A. **19**, 3619 (1986)
40. A. Müller, H.A. Weidenmüller, C.H. Lewenkopf, Europhys. Lett. **22**, 193 (1993)
41. T. Chakraborty, P. Pietiläinen, Phys. Rev. B **50**, 8460 (1994)
42. R.A. Römer, A. Punnoose, Phys. Rev. B **52**, 14809 (1995)
43. A.A. Zvyagin, I.V. Krive, Sov. J. Low Temp. **21**, 533 (1995)
44. B.I. Halperin, Phys. Rev. B **25**, 2185 (1981)
45. C. Cohen-Tannoudji, B. Diu, F. Laloë, *Quantum mechanics*, (Wiley, New York, 1977)
46. C.S. Lent, Phys. Rev. B **43**, 4179 (1991)
47. A. Groshev, I.Z. Kostadinov, I. Dobrianov, Phys. Rev. B **45**, 6279 (1992)
48. R. Courant, D. Hilbert, *Methods of Mathematical Physics*, (Interscience Publications, John Wiley and Sons, New York, USA, 1953)